Wave attenuation by coastal vegetation – An Empirical study on synthetic models

S Hemavathi* & R Manjula

Department of Civil Engineering, National Institute of Technology, Tiruchirappalli (NITT), Tamil Nadu – 620 015, India
*[E-mail: shemathiru@gmail.com]

The interaction between wave and submerged vegetation is the primary cause of wave-induced attenuation. Studies on wave vegetation interactions mostly considered aquatic monotypic plant meadows and limited work have been reported on heterospecific plant meadows, common in tropical shores of southern India. An attempt was made to understand the heterospecific vegetation meadow-wave interactions through a two-level, four factors, full factorial experimental design-based laboratory flume study under controlled conditions. Simulated vegetation mimics were used as a simplified representation of heterospecific seagrass species, *Halophila spinulosa, Halophila ovalis* to develop a linear empirical model. Four input variables *viz.*, water depth *(h)*, wave period *(T)*, plant density *(N)* and bed roughness factor *(f)*, were considered for the study with the wave attenuation (*E* %) as a response. The developed model was tested for adequacy by using the analysis of variance (ANOVA) technique. Main and interaction effects of the input variables were analyzed, compared, and validated. The results show that all the four input variables are statistically significant with the *T* has the highest significant individual effect on wave attenuation followed by *f, h,* and *N*. Evidential two-way interaction effects, mainly between *h* with the rest of the parameters were also observed.

[**Keywords**: Empirical modeling, Plant-flow interactions, Vegetation damping, Wave dissipation, Wave flume study]

Introduction

Coastal vegetation (e.g. seagrass, kelp, mangroves etc.) has been playing a crucial role within the ecosystem by reducing near shore tidal water velocity and hydrodynamic energy[1–4], thereby act as a natural, sustainable coastal protection system. When a wave propagates over aquatic vegetation, and if the water depth is low enough for the oscillatory wave to penetrate the canopy, wave-vegetation interaction generally takes place. The wave forces induce drag and reorientation in vegetation resulting in loss of wave height and energy[5,6]. The degree of attenuation depends mainly on: a) the biophysical plant characteristics such as plant density, plant height, plant stiffness, degrees of freedom, spatial configuration and buoyancy, and b) the hydrodynamic wave parameters such as water depth, wave height, wave period and direction. The variability of wave attenuation is too large such that a general standard procedure for a systematic study on "plant-induced attenuation" has not yet been well established[7].

Several field studies on damping effects due to wave vegetation interactions at different scales are widely documented and quantified in the field[5,8,9] in laboratory flumes[10–12] and numerical models[4]. However, for submerged vegetation, the physical mechanisms which control the wave transformation are not entirely understood, and the influence of control parameters on wave vegetation interactions are inconsistent, for example, the effect of vegetation density on wave height reduction[13].

Earlier researchers focused mainly on measuring wave dissipation within the vegetation[8]. Later, however, comparison studies between vegetated and unvegetated fields gained importance for emphasizing the need for sustainable coastal maintenance and protection. Möller *et al.*[9,14] reported an approximately 50 % increase in wave attenuation from the vegetated field over a mudflat. Bradley & Houser[5] conducted a field study on natural vegetation in shallow waters in North America and reported a strong dependency of wave-vegetation interaction on wave period by calibrating numerical models against observed wave dissipation values without using the actual force on vegetation. Mendez & Losada[7] developed an empirical model for plant induced wave transformations over vegetation canopies at variable water depths.

Most of the published research[5,8–12,15] concentrate on flow-plant interactions over monotypic (composed of organisms of the same type or species) plant meadows. However, heterospecific (an intermixture of underwater pastures) populations of aquatic plant

species[16,17] are widely available in various locations such as Gulf of Mexico, South America Caribbean region, Australia, India, Malaysia, Japan and Thailand[16]. In general, various heterospecific group of plant meadows such as *Cymodocea rotundata*, *Cymodocea serrulate*, *Halodule pinifolia*, *Halodule uninervis*, *Halodule wrightii*, *Halophila beccarii*, *Halophila ovalis*, *Halophila spinulosa*, and *Halophila ovata* generally occur in patches as mixed meadows[16]. Even though there have been several published literatures available on wave attenuation of monotypic plant, studies on heterospecific vegetation are somewhat limited. In addition to the number of wave attenuation studies based on model development and experimentation using idealized homogenous vegetation, several researchers have also performed wave attenuation studies using heterogeneous vegetation[18,19]. Blackmar *et al.*[20] proved from their scaled experiments to evaluate attenuation coefficient for the heterospecific plants from the known coefficients of the individual plants. Nevertheless, in recent times, systematic studies on wave vegetation interaction of heterospecific meadows and the associated effect of control parameters on wave attenuation are gaining importance due to coastal hazards such as the continuous surge storms, cyclones, and the occasional tsunami.

The present study, therefore, investigates the flow-plant interaction effects on heterospecific vegetation during wave attenuation. A two-level, four factors full factorial experimental design was employed to conduct the experiments. An empirical mathematical model was developed from the observed experimental results. The developed model was analyzed by using the analysis of variance (ANOVA) technique, to evaluate the significance of the individual input variables and also to examine their main and interaction effects on wave attenuation. A new set of experiments were carried out to validate the developed model by comparing the predicted results from the model to that of the observed experimental results.

Methodology

Theoretical background

Generally, the wave forces induce 'drag' through the vegetation and re-orient its direction during wave attenuation. This horizontal wave-induced drag attenuates the orbital wave velocities and thus the wave height and energy. It is well-established[21,22] that the wave attenuation by aquatic plants is a function of plant characteristics as well as hydrodynamic conditions. For linear waves, the general formula for the measurement of wave heights when converted into energy density E (J.m^{-2}) is given by

$$E = \frac{1}{8}\rho g H^2 \qquad \qquad \text{... (1)}$$

Where, 'ρ' is the density of seawater, 'g' is the acceleration due to gravity, and 'H' is the wave height. Fonseca & Cahalan[12] calculated the wave energy density reduction using the percent reduction in energy density ($E\%$) over a 1 m test section:

$$E\% = \left[\left\{\frac{E(in)-E(out)}{E(in)}\right\} \times 100\right] \qquad \text{... (2)}$$

Where, $E(in)$ is the energy density entering the 1 m test section and $E(out)$ is the energy density leaving the 1 m test section.

Experimental procedure and measurements

General set-up

Experiments were conducted at the wave flume, National Institute of Technology, Tiruchirappalli (NITT), Tamil Nadu, India. The test scale was 1:1 for providing results unaffected by scale effects. Artificial plant meadow was taken allowing for observations over a short field.

Wave flume set up

The NITT wave flume is 12.5 m long, 0.3 m wide and 0.6 m deep and is equipped with an electro-hydraulic piston wave generator at the left side of the flume. A rubble masonry wave absorber of 1:7 was installed at the opposite of the wave generator for eliminating wave reflection. A 6 m long flat, horizontal area was made in the middle portion of the flume, and a patch of 1m long artificial plant meadow was placed as shown in Figure 1. The simulated canopy started approximately 4 m from the wave paddle.

Heterospecific Halophila species

For the present study, simulated models for heterospecific meadows that comprise two of the major *Halophila* species which include *Halophila spinulosa*, *Halophila ovalis* (schematically shown in Fig. 2), made of plastic were selected for the most similar physical properties to real leaves with $E = 0.9$ GPa. The ρ and E of the plastic material used are 550–700 kg/m^3 and 0.903 GPa, respectively[4].
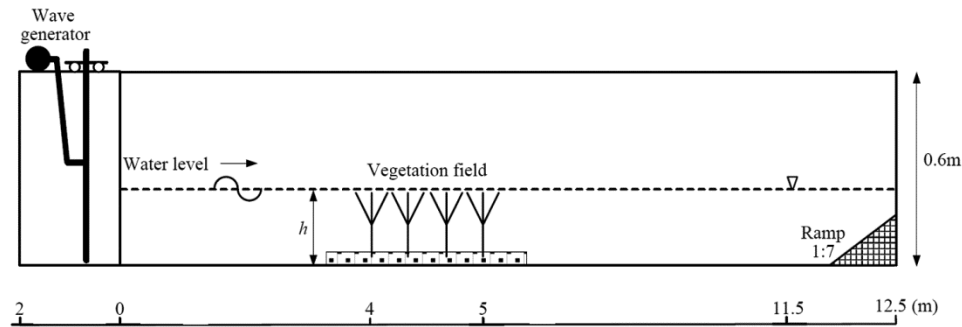
Fig. 1 — Details of the experimental setup

Fig. 2 — Morphological features of synthetic plant species used for the study

The mimics of a typical physical *Halophila spinulosa* has 10-20 pairs of leaves (15-20 mm long and 3-5 mm wide) arranged in opposite per shoot which can be upto 15 cm long. *Halophila ovalis*, on the other hand, has cross veins 8 or more pairs with a 5-40 mm length and 5-20 mm width leaves[23]. The average biomass of the *Halophila* family ranges from 1-46 g dry weight/m^2 and an average density of 15-2855 shoots/sqm[17,24].

The artificial plants for *Halophila ovalis* have 0.01 m × 0.01 m long leaves (Fig. 3). Each simulated plant is composed of 6-10 leaves attached to 0.01 m stems. The *Halophila spinulosa* is represented by 0.003 m diameter plastic stripes of length 0.01 m. Bothmimics were mounted on a 1 m × 0.26 m staggered alternatively in equal distribution on a plastic base
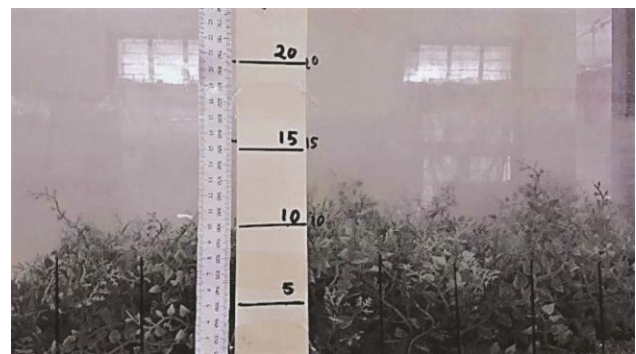

Fig. 3 — The synthetic plant species in the flume under experimentation

plate which was pasted over the metallic flume bed in a staggered placement (spacing 43 mm and 21.5 mm) representing the selected plant densities (543 stems/sqm and 2163 stems/sqm). Regarding the mechanical properties for the model used, the dimensional analysis was performed for determining the specific parameters for using plastic as a material for constructing the artificial heterospecific *Halophila* meadow.

Digital HD Video Camera Recorder SONY, Model No: HDR-PJ50V with a sampling frequency of 25Hz, 1920 × 1080 high definition resolution, was used for observing wave profile. The recorded video images were processed using MATLAB Image processing tool, and the wave profile time series was obtained. For computing wave attenuation, the experimentally measured wave height (*H*) during the entry and exit of the plant meadow was used.

Full factorial experimental design methodology

In a two-level-four-factor (*2^4*) full factorial design, the minimum number of trial runs requires *2^4 = 16* sequences and three replications with a total of 48 runs. Four independent factors, water depth *(h)*, wave period *(T)*, plant density *(N)*, and bed roughness factor *(f)* were considered and studied at two different levels,

represented with a minus sign (-1) as a low and a plus sign (+1) as a high level. The two levels of the selected factors are assumed to have a linear relationship between factor effects at all levels[25]. Table 1 shows the control factors, limits, and symbols used in the experiment. Steel surface and fine sand (mobile condition) were used to represent the lower and higher levels of bed roughness, respectively.

The statistical and graphical analysis of experimental data was performed using Minitab® software release 17, developed by Minitab Inc., USA. Regression analysis for the measured data was performed using this software to identify the main and interaction effects of the selected variables on the predicted response, $E \%$. The general linear regression equation based on the first-order model with the selected four parameters and all their two-way interaction terms are in the form of the following equation:

$$Y = \beta_0 + \sum_{i=1}^{k} \beta_i X_i + \sum_{1 \leq i \leq j}^{k} \beta_{ij} X_i X_j + \varepsilon \qquad \dots (3)$$

Where Y is the predicted response, k is the number of factors, β_0 is the constant term, β_i is the linear coefficient representing the effect of the factor, β_{ij} represents the interaction effects, X_i and X_j are the independent coded variables, and ε is the experimental error. The linear regression equation was obtained using the coded independent parameters like the following:

$$\begin{aligned} E\% = \beta_0 &+ \beta_1\, h + \beta_2\, T + \beta_3\, N + \beta_4\, f + \beta_{12} h * T \\ &+ \beta_{13}\, h * N + \beta_{14} h * f + \beta_{23}\, T * N \\ &+ \beta_{24}\, T * f + \beta_{34} N * f + \beta_{123}\, h * T \\ &* N + \cdots \end{aligned}$$
$$\dots (4)$$

Where, $E\%$ is the energy reduction percentage, β_0, β_1, β_2, β_3, β_4 are the linear coefficients, and β_{12}, β_{13}, β_{14}, β_{23}, β_{24}, β_{34} are the second order interaction terms and so on.

Results and Discussions

Modeling and statistical analysis

For the collected experimental data, regression analysis was conducted to fit a linear model using the least square technique. The developed mathematical model for predicting the percentage of wave energy reduction density ($E\%$) from the design matrix-based experimentation results is expressed using real factors as follows:

$$\begin{aligned} E\% = 37.372 &- 5.401h - 18.212T + 2.279N + \\ 8.495f &+ 21.754\, h * T - 3.938\, h * N - 4.445\, h * \\ f &+ 0.933\, T * N + 0.970\, T * f - 8.778\, N * f - \\ 5.230\, &h * T * N - 6.140\, h * T * f + 5.018\, h * N * \\ f &- 8.479\, T * N * f + 1.588\, h * T * N * f \quad \dots (5) \end{aligned}$$

The main effects of the factors were distinguished by the statistical significance of fitted models based on the Fisher's test (p-value < 0.05) of confidence intervals using the analysis of variance (ANOVA) technique[25]. The statistically insignificant main, two-way interaction variables whose p-values are more than 0.05 (at 95 % confidence level) neglected along with all the three-way interaction variables, the selected model is given by:

$$\begin{aligned} E\% = 37.372 &- 5.401h - 18.212T + 2.279N + \\ 8.495f &+ 21.754h * T - 3.938h * N - 4.445\, h * f - \\ 8.778\, &N * f \qquad \dots (6) \end{aligned}$$

The fitted model was analyzed by identifying the adequacy of the developed model and error independency for each selected variable in the study. The adequacy and the significance of each coefficient for the developed model were too tested by applying the ANOVA technique. The standard error (SE) of the estimated coefficient of all possible correlations and the coefficient of determination value (R^2) for all main and two-way interaction effects derived from the regression analysis are given in Table 2.

From the regression analysis, based on the p-values (< 0.05), it was found that all the individual factors (h, T, N, and f) in the model have significant effects individually as well as in combination among each other on $E\%$ as the response. For the validation of the developed regression model, a new set of experiments were conducted under similar experimental conditions. The collected data experimental results were plotted against the corresponding predicted data

Table 1 — Control factors and their limits

Factors	Unit	Symbol	Coded symbol	The actual value of coded levels	
				Low (-1)	High (+1)
Water depth	m	h	β_1	0.10	0.15
Wave period	s	T	β_2	1.0	3.0
Plant density	stems/sqm	N	β_3	543	2163
Bed roughness factor	-	f	β_4	0.012	0.018

Table 2 — ANOVA results for $E(\%)$ loss

Source	Sum of Squares	Degree of Freedom	Mean square	F_p Value	p-value Prob $> F_p$
Model	21034.6	4	5258.6	295.41	< 0.0001
A - h	1400.2	1	1400.2	78.66	< 0.0001
B - T	15921.0	1	15921.0	894.36	< 0.0001
C - N	249.3	1	249.3	14	0.001
D- f	3464.1	1	3464.1	194.6	< 0.0001
AB	22715.7	1	22715.7	1276.05	< 0.0001
AC	744.2	1	744.2	41.81	< 0.0001
AD	948.4	1	948.4	53.27	< 0.0001
BC	41.8	1	41.8	2.35	0.135
BD	45.1	1	45.1	2.53	0.121
CD	3698.6	1	3698.6	207.77	< 0.0001
Pure Error	569.6	32			
Total	57701.0	47			

R^2(Adequate) = 0.9801 %, R^2(Adjusted) = 0.9855, R^2(Predicted) = 0.9778
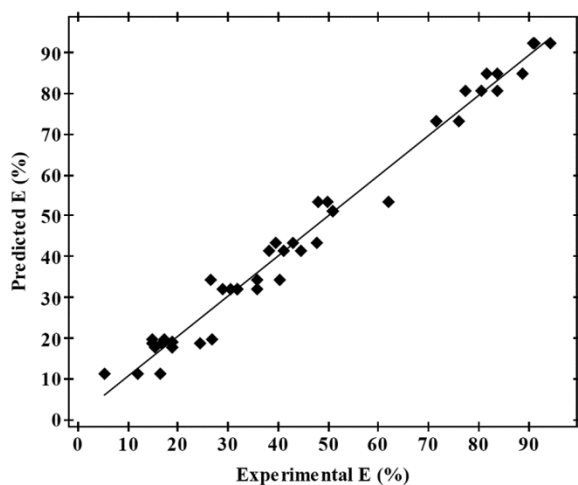df degrees of freedom, F_p Fisher's ratio, p - probability

Fig. 4 — Comparison between predicted and experimental $E\%$

generated from the developed regression model and is graphically shown in Figure 4. Each predicted value from the developed model matches its newly observed experimental results well.

Main Effects of tested variables on $E\%$

The graphical plots of the main effects of all the statistically significant tested variables on $E\%$ are given in Figure 5(A-D). The graphs illustrate that the water depth h and wave period T have an opposite effect while plant density N and bed roughness factor f both have a direct impact on $E\%$. Among all the four statistically significant parameters, the intensity of the individual impact is high for T (-ve) and f (+ve) as compared to h (-ve) and N (+ve). The main effect of each of the statistically significant tested variables is discussed in the following section.

Effect of water depth

The water depth plays a vital role in wave attenuation[12,26,27] although it was reported[21] that its influence is comparatively less clear than other parameters such as wave period, stem density, etc. The present study confirms the importance of wave depth on wave attenuation (Fig. 5A). When h increases from 0.1 m to 0.15 m, $E\%$ reduces from 43 % to 32 %. This inverse relationship between water depth and wave energy reduction has been widely recognized[21]. The individual effect of water depth is generally identified based on the determination of the submergence ratio, the ratio of stem length (ls) to water depth (h)[13,26]. It was agreed that a lower submergence ratio leads to higher wave dissipation[28–30]. For the present study, higher wave reduction was observed at the lower limit of the water depth (0.1 m) when the plant mimics were under emergent condition ($ls/h \geq 1.0$), while at the higher limit the wave dissipation was decreasing as plant mimics were under submerged condition (water depth exceeded canopy height, $ls/h < 1.0$). Fonseca & Cahalan[12] also reported a wave height attenuation between 20 % and 76 % ($\approx$ 40 % on average) over 1m length for four common sea grass plants under near emergent condition. However, Augustin et $al.$[10] reported much higher wave attenuation per wavelength over the emergent plant (50-200 %) than near emergent ($ls/h = 0.75$) stems. The results from the present study, therefore, is in good agreement with the published results[10,12,31] and confirms that during low tides, when water depths are shallow enough, the advancement of waves over a vegetated surface
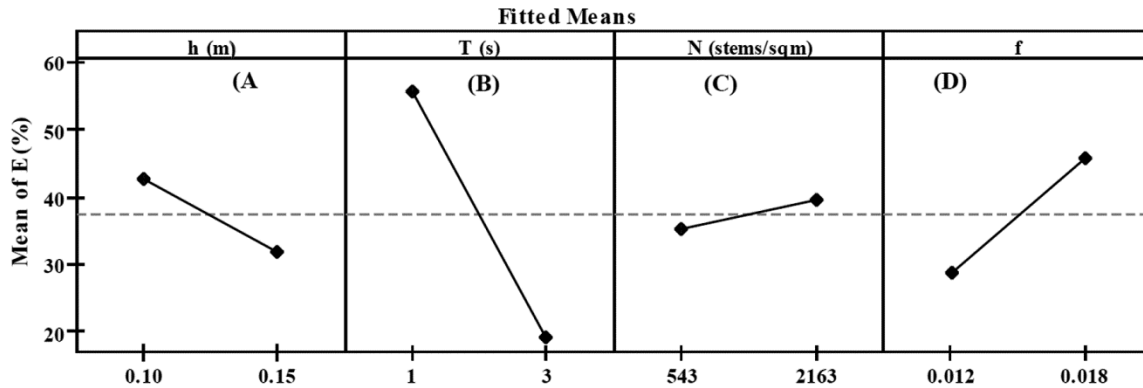
Fig. 5 — Main effects of tested variables on *E%*

results in high wave-vegetation interactions-based flow resistance.

Effect of wave period

The plot, Figure 5(B) represents that an increase of wave period *T*, and therefore of the wavelength results in a higher reduction of *E%* (more than 30 %) along the meadow between the tested wave periods (1 to 3 s). The wave attenuation is reduced for the lower *T*, as the reduction of the wave height along the meadow reaches approximately from 82 % to as low as 30 % behind the field for the considered wave periods.

Effect of plant density

From Figure 5(C), observation indicates when *N* increases from 543 stems/sqm to 2163 stems/sqm, the *E%* increases from ≈ 35 to 40 %. This result is in good agreement Bouma *et al.*[28]; however, the effect of plant density on wave-vegetation interactions are still not apparent. Some studies observed an improved wave dissipation due to higher plant density[28] and others found that it does not affect[10,12] and it is generally agreed that wave dissipation is related to shoot stiffness[28] and plant morphology[32].

Effect of the bed roughness factor

The main effect plot, Figure 5(D) shows that an increase in f from the smooth metallic flume bed (0.012) to the sandy flume bed (0.018), the E% increases from ≈ 29 to 46 %. Generally, wave friction factors at the bed (f_w) have been stated as a function of the orbital wave amplitude (A) and the hydraulic roughness (r). The r is related to the geometry of the roughness elements and the vertical length scale of the wave boundary layer. Modelling vegetation roughness through the use of a dimensionless friction factor was found to provide a reasonable estimate for the amount of wave attenuation that may occur through vegetation fields. Generally, empirical equations are derived for obtaining the friction factor(f_w) to avoid the necessity of field data. For fully-rough turbulent flows, the widely used empirical equation by Paul & Amos[27] to calculate f_w is given by:

$$f_w = exp\left[5.5\left(\frac{r}{A}\right)^{0.2} - 6.3\right] \qquad ... (7)$$

Where, r is hydraulic roughness and A is orbital wave amplitude.

Equation (7) shows that the wave friction factor at the bed (*f_w*), is exponentially increased by the value of *r* although its application to flexible vegetation is unproven[27]. In the present study, *r* is equivalent to the roughness factor *f*, which means an increase in *r* will consequentially increase the *E%*.

Interaction effects of tested variables on *E%*

Figure 6(A-F) shows the combined interaction effects among all the tested variables on *E%* over the vegetation meadow. The interactions of *h* with *T*, Figure 6(A), *h* with *N*, Figure 6(B), *h* with *f*, Figure 6(C) and *N* with *f*, Figure 6(F) are statistically significant and are discussed in the following section. The interaction of *T* with *N*, Figure 6(D) and *f*, Figure 6(E) are statistically insignificant, on their effect on *E%* and are neglected.

Interaction effect of *h* with *T*

Numerous flume, field and modeling studies[5,27,33–35] confirmed the dependency of wave-vegetation interactions on wave period with a different noticeable trend in results. Field measurements from Infantes *et al.*[36] showed higher dissipation for more extended wave periods, whereas Anderson & Smith[21] indicated the opposite. For the present study, Figure 6(A) shows that the interaction effect of water depth
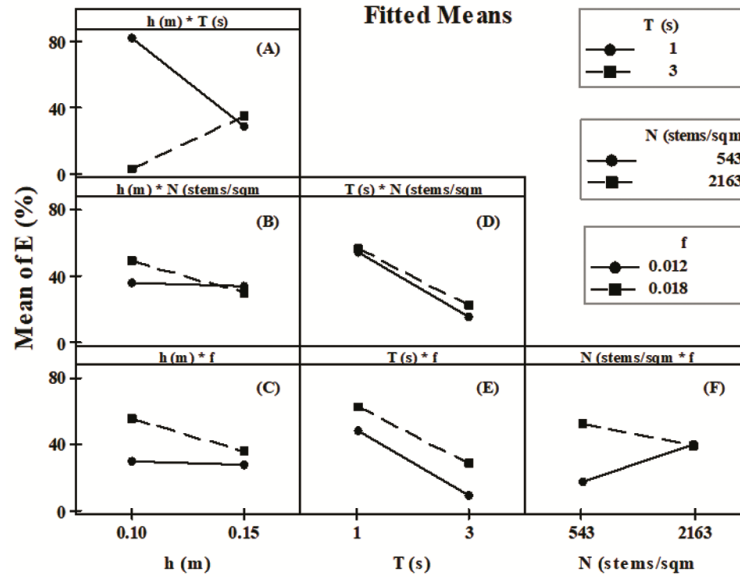
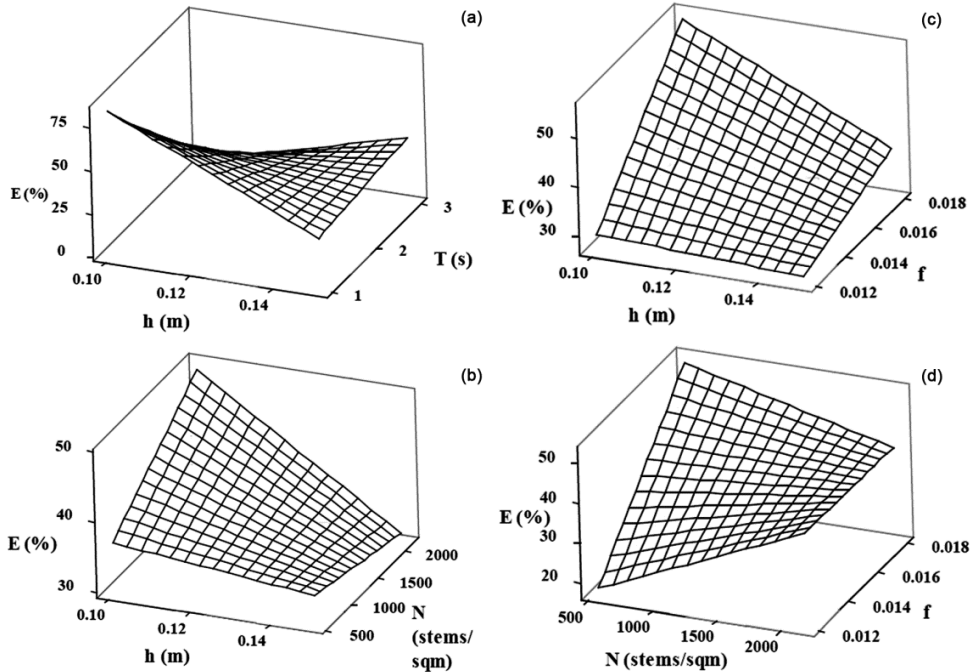Fig. 6 — Two-way interaction effects of tested variables on $E\%$

Fig. 7 — Surface plot for the Interaction effect of: a) h and T on $E\%$; b) h and N on $E\%$; c) h and f on $E\%$; and d) N and f on $E\%$

h causes a decrease in $E\%$ for the lower T with the highest reduction when both h and T are of the lowest range, which can further be demonstrated in a three-dimensional surface plot shown in Figure 7(a). The lowest water depth (0.10 m) at the shorter wave period (1 s) results in high wave energy reduction percentage (75 %).

However, the same water depth (0.10 m) at the longest wave period (3 s) results in the lowest level

$E\%$ (15 %). On the contrary, the highest water depth (0.15 m) at the shorter wave period (1 s) results in lower $E\%$ (25 %) but, lowest water depth (0.10 m) at the prolonged wave period (3 s) results in comparatively higher wave energy reduction percentage ($\approx$53 %). Among all the process control parameters considered in this study, the effect of wave period on dissipation has had the most contradictory results from the literature. Möller et al.[14] reported that

salt marshes reduced wave energy at all wave periods by the same degree as compared to the flat sand bottom-based flows. But other studies[5,35] suggested that the vegetation-based wave attenuation is predominantly high wave period (high-frequency) dependent. These contradictory results are attributed to the interaction effect of water depth, demonstrated in the present study.

Some researchers[12,32] considered wave period as a function of water depth by using wavelength L to define the relative water depth (h/L) so as to specify whether a wave in a shallow water (h/L < 0.05), intermediate (0.05 < h/L < 0.5), or deep water (h/L > 0.5). By this consideration, the decreasing of wave attenuation observations can be explained regarding waves approaching of the deep-water regime as waves interact with the bottom, based on relative depth, so waves with longer wavelengths become shallow-water waves and interact with the bed at deeper depths[32]. Stratigaki et $al.$[26] reported more than a 35 % reduction of wave height along the meadow due to a decreasing of the wave period. The interaction effect between h and T on E% along the vegetation meadow from the present study, therefore is one of the reasons for the contradictory results from the previous studies Figure 6(A).

Interaction effect of h with N

Several published results[28–30] suggested that there have been significant interactions between lower h and higher N, that are responsible for a higher degree of wave attenuation. The results of the present investigation, Figure 6(B) hence demonstrated good agreement with such interaction effects of low h and N on $E\%$ reduction. When combined, h and N made an opposite effect on $E\%$ during an increase from lower to higher limits of each other. However, as h increases from 0.1 m to 0.15 m, additional N has a more pronounced reduction of the $E\%$ (more than 18 %), while low N has a considerably lesser impact on $E\%$ (around 3 %). An increase of the h from 0.1 m to 0.15 m therefore, results in a higher reduction of energy loss along the meadow, between the tested plant densities. The three-dimensional surface plot shown in Figure 7(b) demonstrated that the highest reduction in $E\%$ is achievable when the h is minimum and with maximum N[28].

For the present study, the close arrangement of the heterospecific mimics suggests that plants within the canopy patch interact with each other in the cross-stream direction. Since the shoots of different wave facing frontal areas are arranged too close to each other, the turbulence at their edges might affect neighboring plants and increases the drag force acting on them. It was reported[37] that higher stem densities resulted in more significant attenuation, both at high and low water depths which is in good agreement with the results from the present study.

Interaction effect of h with f

The significance of h and f interactions in wave attenuation graphically demonstrated in Figure 6(C) shows that when h is at the lower level (0.1 m), the change in flume bed roughness factor from 0.012 (metallic flume bed) to 0.018 (sandy flume bed) results in around 26 % increase in E%. However, an increase in water depth from 0.10 m to 0.15 m with the change in bed roughness causes an increase in E% to a marginal 7 %. Also, the drop in E% due to variation in water depth from 0.10 to 0.15 m during the sandy bed flume (0.018) based wave flow is 20 % as compared to the metallic bed flume wave flow (0.012) of 1 %. This result is also analogous to the findings from unidirectional flow studies[38,39]. The higher the proportion of the water depth over the canopy, the less effective it is at reducing unidirectional flows which can further be demonstrated in a three-dimensional surface plot shown in Figure 7(c).

Interaction effect of N and f

Statistically significant two-way interaction effect has been observed between the bed roughness factor, f and the plant density, N on E%, which is demonstrated graphically in Figure 6(F). For a lower N, change of f from 0.012 (metallic flume bed) to 0.018 (sandy flume) causes an increase in an energy reduction of about 35 % and high rise in wave attenuation is attributable to the plant density since flat metallic flume bed induces less friction. This result is analogous to results from many studies[26,33,37].

However, a change in f from 0.012 (metallic flume bed) to 0.018 (sandy flume) causes the almost same amount of E% reduction (about 40 %) between the tested N. Moreover, the low roughness factor 0.012 (metallic flume bed) causes an increase in E% reduction (≈22 %) while high roughness factor related to the sandy flume, 0.018 causes a marginal decrease in E%. The surface plot, Figure 7(d), shows that the plant density increase at higher bed roughness does not enhance the attenuation. It is important to note that the bed roughness is an important parameter,

capable of modifying the hydrodynamic environment and causing wave attenuation, particularly for small-orbital amplitude waves and at low Reynolds numbers.

Conclusion

This study was carried out to understand the influence of wave damping control variables such as water depth (h, 0.1–0.15 m), wave period (T, 1–3 s), plant density (N, 543–2163 stems/sqm) and bed roughness factor (f, 0.012–0.018) of heterospecific seagrass meadow based on a two-level, four factors full factorial design of experiments (DOE) methodology. Two replicated experiments were conducted to develop a linear regression model from the experimental results to predict $E\%$ as the response variable and the model was tested for adequacy using the ANOVA technique. The results indicated that all the four input variables h, T, N, and f are statistically significant with h and T to have a negative effect whereas N and f have a positive effect on the response $E\%$. Statistically, significant two-way interaction effects between h-T, h-N, h-f, and N-f were also observed. The analysis of variance (ANOVA) results indicated that the regression model is statistically significant with a high coefficient of determination (R^2) of 0.9801 and p-value < 0.05. To compare and validate the efficacy of the developed model, a new set of experiments were conducted at similar experimental conditions. The results confirmed that the developed factorial regression model is reasonably accurate in predicting wave attenuation with an error percentage less than 5 % and that the technique has proven to be very effective for identifying the statistical significance of the input variables such that the mathematical modelling could be explored using non-linear modelling for further study.

Acknowledgments

Conflict of Interest

The authors with this confirm that there are no known conflicts of interest associated with this research work.

Author Contributions

Conceptualization and design of the work: SH and RM. SH: Conceptualization, methodology, data collection, analysis, interpretation of data, software, prepared manuscript. RM: Supervised the whole research, resources, review and corrected the manuscript.

References

1   Möller I, Kudella M & Rupprecht F, Wave attenuation over coastal salt marshes under storm surge conditions, *Nat Geosci*, 7 (2014) 727–731.

2   Xu S, Liu Y, Wang X & Zhang G, Scale effect on spatial patterns of ecosystem services and associations among them in semi-arid area: A case study in Ningxia Hui Autonomous Region, China, *Sci Total Environ*, 598 (2017) 297–306.

3   3Specht A, Gordon I J, Groves R H, Lambers H & Phinn S R, Catalysing transdisciplinary synthesis in ecosystem science and management, *Sci Total Environ*, 534 (2015) 1–3.

4   Koftis T, Prinos P & Stratigaki V, Wave damping over artificial Posidonia oceanica meadow: A large-scale experimental study, *Coast Eng*, 73 (2013) 71–83.

5   Bradley K & Houser C, Relative velocity of seagrass blades: Implications for wave attenuation in low-energy environments, *J Geophys Res Earth Surf*, 114 (2009) 1–13.

6   Dalrymple R A, Kirby J T & Hwang P A, Wave Diffraction Due to Areas of Energy Dissipation, *J Waterw Port, Coastal, Ocean Eng*, 110 (1984) 67–79.

7   Mendez F J & Losada I J, An empirical model to estimate the propagation of random breaking and nonbreaking waves over vegetation fields, *Coast Eng*, 51 (2004) 103–118.

8   Knutson P L, Brochu R A, Seelig W N & Inskeep M, Wave damping inSpartina alterniflora marshes, *Wetlands*, 2 (1982) 87–104.

9   Möller I & Spencer T, Wave dissipation over macro-tidal saltmarshes: Effects of marsh edge typology and vegetation change, *J Coast Res*, 36 (2002) 506–521.

10   Augustin L N, Irish J L & Lynett P, Laboratory and numerical studies of wave damping by emergent and near-emergent wetland vegetation, *Coast Eng*, 56 (2009) 332–340.

11   Hu Z, Suzuki T, Zitman T, Uittewaal W & Stive M, Laboratory study on wave dissipation by vegetation in combined current-wave flow, *Coast Eng*, 88 (2014) 131–142.

12   Fonseca M S & Cahalan J A, A preliminary evaluation of wave attenuation by four species of seagrass, *Estuar Coast Shelf Sci*, 35 (1992) 565–576.

13   Manca E, Cáceres I, Alsina J M, Stratigaki V, Townend I, *et al*., Wave energy and wave-induced flow reduction by full-scale model Posidonia oceanica seagrass, *Cont Shelf Res*, 50 (2012) 100–116.

14   Möller I, Spencer T, French J R, Leggett D J & Dixon M, Wave transformation over saltmarshes: a field and numerical modelling study from North Norfolk, England, *Estuar Coast Shelf Sci*, 49 (1999) 411–426.

15   Koftis T & Prinos P, Estimation of wave attenuation over Posidonia Oceanica, *Appl Coast Research*, 4 (2014) 1-8.

16   Kuo J & den Hartog C, Taxonomy and Biogeography of Seagrasses, In: *Seagrasses: Biology, Ecology, and Conservation*, (Springer, Netherlands), 2006, pp. 1–23.

17   Jagtap T G, Komarpant D S & Rodrigues R, *Seagrasses of India: World Atlas of Seagrasses*, edited by E P Green & F T Short, 2003, pp. 101–108.

18 Chang C W, Liu P L F, Mei C C & Maza M, Periodic water waves through a heterogeneous coastal forest of arbitrary shape, *Coast Eng*, 122 (2017) 141–157.

19 Chang C W, Liu P L F, Mei C C & Maza M, Modeling transient long waves propagating through a heterogeneous coastal forest of arbitrary shape, *Coast Eng*, 122 (2017) 124–140.

20 Blackmar P J, Cox D T & Wu W C, Laboratory observations and numerical simulations of wave height attenuation in heterogeneous vegetation, *J Waterw Port*, *Coast Ocean Eng*, 140 (2014) 56–65.

21 Anderson M E & Smith J M, Wave attenuation by flexible, idealized salt marsh vegetation, *Coast Eng*, 83 (2014) 82–92.

22 Nobuhisa K, Raichle A W & Asano T, Wave attenuation by vegetation, *J Waterway Port Coastal Ocean Eng*, 119 (1) (1993) 30–48.

23 Mckenzie L, Seagrass Educators Handbook, *Seagrass-Watch*, 20 (2008).

24 El Shaffai A, *Field Guide to Seagrasses of the Red Sea Gland*, IUCN, Switzerland, 2011.

25 Montgomery D C & Runger G C, Applied statistics andprobability for engineer, *Eur J Eng Educ*, 19 (3) (1994) 383.

26 Stratigaki V, Manca E, Prinos P, Losada I J, Lara J L, *et al.*, Large-scale experiments on wave propagation over Posidonia oceanica, *J Hydraul Res*, 49 (2011) 31–43.

27 Paul M & Amos C L, Spatial and seasonal variation in wave attenuation over Zostera noltii, *J Geophys Res Ocean*, 116 (2011) 1–16.

28 Bouma T J, De Vries M B, Low E, Peralta G, Tánczos I C, *et al.*, Trade-offs related to ecosystem engineering: A case study on stiffness of emerging macrophytes, *Ecology*, 86 (2005) 2187–2199.

29 Huang Z, Yao Y, Sim S Y & Yao Y, Interaction of solitary waves with emergent, rigid vegetation, *Ocean Eng*, 38 (2011) 1080–1088.

30 Paul M, Bouma T J & Amos C L, Wave attenuation by submerged vegetation: Combining the effect of organism traits and tidal current, *Mar Ecol Prog Ser*, 444 (2012) 31–41.

31 Dubi A & Alf Torum, Wave Energy Dissipation in Kelp Vegation, *Coast Eng*, (1996) 2626–2639.

32 Koch E W, Sanford L P, Chen S N, Shafer D J & Smith J M, Waves in seagrass systems: review and technical recommendations (ERDC-TR-06-15), 12 (2006) 5-92.

33 Mullarney J C & Henderson S M, Wave-forced motion of submerged single-stem vegetation, *J Geophys Res Ocean*, 115 (2010) 1-14.

34 Jadhav R S, Chen Q & Smith J M, Spectral distribution of wave energy dissipation by salt marsh vegetation, *Coast Eng*, 77 (2013) 99–107.

35 Lowe R J, Falter J L, Koseff J R, Monismith S G & Atkinson M J, Spectral wave flow attenuation within submerged canopies: Implications for wave energy dissipation, *J Geophys Res Ocean*, 112 (2007) 1–14.

36 Infantes E, Orfila A, Simarro G, Terrados J, Luhar M, *et al.*, Effect of a seagrass (Posidonia oceanica) meadow on wave propagation, *Mar Ecol Prog Ser*, 456 (2012) 63–72.

37 Tschirky P, Hall K & Turcke D, Wave attenuation by emergent wetland vegetation, *Coast Eng*, (2001) 865–877.

38 Fonseca M S, Fisher J S, Zieman J C & Thayer G W, Influence of the seagrass, Zostera marina L., on current flow, *Estuar Coast Shelf Sci*, 15 (1982) 351–364.

39 Fonseca M S & Koehl M A R, Flow in seagrass canopies: The influence of patch width, *Estuar Coast Shelf Sci*, 67 (2006) 1–9.